Freegah, Basim, Asim, Taimoor and Mishra, Rakesh

Effect of solar heat flux and thermal loading on the flow distribution within the riser pipes of a closed-loop solar thermo-syphon hot water system

28th International Congress of Condition Monitoring and Diagnostic Engineering
10th Regional Congress on Non Destructive and Structural Testing

Effect of solar heat flux and thermal loading on the flow distribution within the riser pipes of a closed-loop solar thermo-syphon hot water system

Basim Freegah[a,b], Taimoor Asim[b] and Rakesh Mishra[b]

[a]*Al-Mustansiriya University, Baghdad, Iraq*
[b]*University of Huddersfield, Queensgate, Huddersfield, HD1 3DH UK*

ABSTRACT- Solar energy is one of the main sources of renewable energy that is abundantly available throughout the world. Solar energy can be used for useful purposes through a number of mechanical artefacts. One such artefact is known as Thermo-syphon, which typically contains water as its working fluid. One of the major applications of Thermo-syphon is within the residential and industrial units, where a constant supply of hot water is required. The use of Computational Fluid Dynamics (CFD) based solvers has recently been proven capable of predicting the flow behaviour within thermo-syphons with reasonable accuracy. Hence, the present study focuses on using a commercial CFD based solver to predict the flow behaviour within the riser pipes of a thermo-syphon with varying solar heat flux and thermal loading conditions. In order to qualitatively and quantitatively analyse the flow structure within the riser pipes of the thermo-syphon, velocity magnitude and static temperature distributions within these pipes is analysed in detail. The results depict that the solar heat flux has a significant impact on the velocity magnitude and static temperature profiles within the riser pipes. Furthermore, it has been observed that the thermal loading has negligible effects on the velocity magnitude and static temperature profiles within the riser pipes. The data has also been used to develop novel design correlations.

Keywords*:* Velocity Magnitude, Static Temperature, Computation Fluid Dynamics (CFD), Closed-loop Thermo-syphon, Solar Energy

1. Introduction

Natural convection phenomenon within the riser pipes of a closed thermo-syphon occur due to the variations in the density of the working fluid, generating buoyant forces. The temperature of the working fluid increases due to the exposed riser pipes collecting solar heat flux. Temperature difference within the working fluid causes a density difference which leads to natural circulation of the working fluid. Many researchers have analysed the effects of different parameters, such as geometric parameters, heat flux input, thermal loading conditions, types of working fluids etc., on the performance characteristics of thermo-syphons. Dehdakhel.et al. (1) carried out experimental studies to analyse the effects of fill ratio on performance of a thermo-syphon for three different heat fluxes. The results have shown that the performance of a thermo-syphon gets significantly affected by the fill ratio. Further CFD study predicts that the temperature profiles within the thermo-syphon match closely with the experimental data.

Freegah et al. (2) conducted numerical studies in order to analyse the effects of collector tilt angle, number of riser pipes, heat flux input and the length-to-diameter ratio of the riser pipes, under no-load condition. The study shows that the angle of inclination has negligibly small effect, while both the heat flux and the length-to-diameter ratio of the riser pipes have significant effects on the performance of a thermo-syphon. Furthermore, increase in the number of riser pipes increases the temperature of the working fluid. Sato et al. (3) conducted theoretical studies in order to analyse the effects of heat pipe tilt angle and condenser geometry on the temperature of the working fluid within the condenser. The study shows that the tilt angle has negligible effects, and that the conventional solar collector geometry is optimal as far as the performance of the thermo-syphon is concerned. Subramanian et al. (4) studied the impact of riser arrangement (zigzag pattern) on the performance of a flat plate solar collector system, and compared it with the conventional system. Experiments have been conducted using copper tubes in header and riser having various geometrical characteristics. The results show that the performance efficiency reached 62.9% in the zigzag arrangement.

Esen et al. (5) experimentally studied three refrigerants i.e. R-134, R-407 and R-410, used as working fluid in a thermo-syphon. The three systems have been tested under the same working conditions in an attempt to determine the most effective refrigerant among the three. The results show that using R-410 as the working fluid is more efficient than other refrigerants, for both the loaded and no-load operations. Radhwan et al. (6) conducted experimental studies on two integrated solar water heaters for both forced and natural circulation water systems. R-11 has been used as the working fluid. The results show that the natural circulation of water has a remarkable impact on the thermal performance, while the forced circulation has relatively weaker impact. Agarwal et al (7). problems of fluid flow within the pipe have been solved using Computational Fluid Dynamics techniques.

It has been noticed from the review of the published literature that the current knowledge base regarding the flow diagnostics within a thermo-syphon lacks in critical understanding of the flow velocity and temperature variations within the riser pipes. This information is of utmost importance to the thermo-syphon designers. Furthermore, the practical use of thermo-syphon involves a broad range of operating conditions in which the heat flux input and the thermal loading conditions constantly vary.

In the present study, detailed numerically investigations have been conducted on the velocity magnitude and static temperature profiles of the working fluid within the riser pipes of a thermo-syphon, for a wide range of operating conditions. This is considered on the basis of day-to-day operations, and hence provides a measure of suitability of choice for effective usage.

2. NUMERICAL MODELLING

2.1. Geometry

Three-dimensional computational domain of a closed-loop thermo-syphon has been created for the numerical simulations. The geometry consists of several riser pipes connected, at the upper end, to the upriser, and at the lower-end to the downcomer, as shown in figure 1. The riser pipes have an internal diameter of 20mm, with a wall thickness of 1mm, whereas the internal diameter of upriser and the downcomer is 25mm, with a wall thickness of 1mm. In the present study, the length-to-diameter ratio of the riser pipes is 50. Furthermore, the diameter of the condenser is five-times the diameter of the riser pipes. The thermo-syphon model has been tilted by 53° to the horizontal, as it is equivalent to the latitude site angle of Huddersfield (UK).

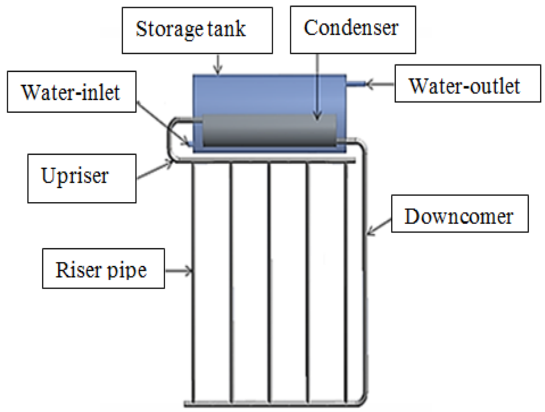

Figure 1. Thermo-syphon Model

2.2. Meshing of the Flow Domain

Hybrid mesh has been employed, using both hexagonal and tetrahedral elements, in the present study. Non-uniform mesh distribution has been used, where the mesh elements have been concentrated in near-wall regions. Five layers of structured hexahedral mesh elements have been generated in near-wall regions with a growth factor of 1.2. This has been specified in order to accurately resolve the boundary layer forming on the walls. The flow domain contains one million mesh elements, which has been previously shown by J Hu et al. (8) to describe the flow phenomena with reasonable accuracy.

2.3. Boundary conditions

Two transient boundary conditions have been used, namely i) heat flux input and ii) thermal loading. Heat flux exposed to the riser pipes has been calculated using equation 1, while thermal loading data has been obtained from N Aung et al. (9).

$$q = I_o\, \varepsilon\tau[\sin\delta\sin(\theta-\propto) + \cos\delta\cos(\theta-\propto)\cos\phi] \quad (1)$$

where I_o is solar radiation intensity, δ is the inclination angle and ϕ is the hour angle which can be calculated using equations provided by ASHRAE (10).

$$\varepsilon = \left[1 + 0.033\ cos\left(\frac{360N_d}{365}\right)\right] \quad (2)$$

where ε denotes the correction factor of the earth's orbit, N_d denotes the day number of the year, and τ denotes the atmospheric transmittance. The τ values vary, with the location and elevation, between 0 and 1, according to Z Sen (11). τ may be as high as 0.8 for clear sky, and may be as low as 0.4 when turbidity is very high.

Using multiple regression analysis on the data generated from equation (1) for heat flux, three equations have been developed for heat flux measurement (corresponding to 15th of March, 15th of June and 15th of September). Chi-square values of these equations are 0.012, 0.009 and 0.009 respectively. Thermal loading data has been obtained from N Aung et al. (9), and two equations to measure the transient thermal loading (representing weekday and weekend loading conditions) have been developed. Chi-square values of these equations are 0.03 and 0.02 respectively, hence the equations developed here depict no significant difference to the available data.

Table 1. Set of equations for heat flux and thermal loading

Type	Equation	Chi-square (p value)	Data
Heat Flux	$HF = HF_{max}\left[3.702\left(t/t_{max}\right)^4 - 6.381\left(t/t_{max}\right)^3 + 0.472\left(t/t_{max}\right)^2 + 1.949\left(t/t_{max}\right) + 0.453\right]$	1	15th March
	$HF = HF_{max}\left[2.484\left(t/t_{max}\right)^4 - 4.281\left(t/t_{max}\right)^3 - 0.103\left(t/t_{max}\right)^2 + 1.667\left(t/t_{max}\right) + 0.556\right]$	1	15th June
	$HF = HF_{max}\left[3.674\left(t/t_{max}\right)^4 - 6.333\left(t/t_{max}\right)^3 + 0.494\left(t/t_{max}\right)^2 + 1.913\left(t/t_{max}\right) + 0.461\right]$	1	15th September
Thermal Loading	$TL = TL_{max}\left[-4.173\left(t/t_{max}\right)^4 + 8.06\left(t/t_{max}\right)^3 - 4.22\left(t/t_{max}\right)^2 - 0.192\left(t/t_{max}\right) + 0.995\right]$	0.99	Working Day
	$TL = TL_{max}\left[0.887\left(t/t_{max}\right)^4 - 0.55\left(t/t_{max}\right)^3 - 1.62\left(t/t_{max}\right)^2 + 0.797\left(t/t_{max}\right) + 0.997\right]$	0.99	Week End

where HF and TL corresponds to heat flux and thermal loading.

3. RESULTS AND ANALYSIS

The thermo-syphon model considered in the presented study has been analysed under various transient heat flux inputs and thermal loading conditions. The following sections describe the variations in velocity magnitude and static temperature profiles of the working fluid within the riser pipes.

3.1. Effect of heat flux input on the performance of thermo-syphon

Figure 2 depicts the flow velocity variations within the cross-section of the middle riser pipe, for the three days of the year considered in the present study. The corresponding thermal loading condition that has been specified is that of the weekday. The scale of the contours has been kept constant for effective comparison purposes. It can be clearly seen that the flow velocity is considerably higher on the upper section of the riser pipe. This is because the hot water rises up in the riser pipe's cross sections, and then propagates towards the upriser. Furthermore, it can be clearly seen that the velocity within the riser pipe is highest on 15th of June as compared to 15th of March and 15th of September. This means that the working fluid's velocity increases significantly on the days when the heat flux input to the thermo-syphon is higher.

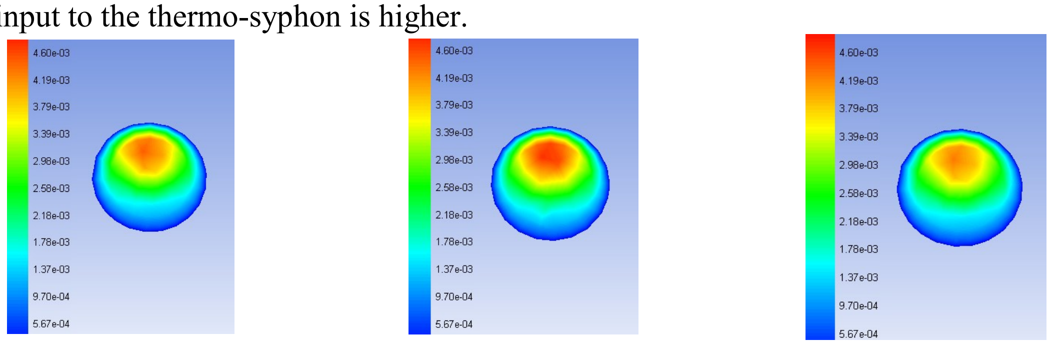

(a) (b) (c)

Figure 2. Flow velocity variations within the middle riser pipe on (a) 15th of March (b) 15th of June (c) 15th of September under thermal loading of a working day

Figure 3 depicts the velocity profiles of the working fluid within the middle riser pipe for the three different days of the year considered in the present study, under working day thermal loading conditions. It can be clearly seen that the velocity of the working fluid is higher at the center of riser pipe for all cases. Furthermore, increase in heat flux input increases the velocity of working fluid within the riser pipe. It can be further seen that the flow of the working fluid within the riser pipe is fully developed.

Figure 4 depicts the variations of Reynolds Number (Re) of the working fluid within the cross-section of the middle riser pipe for the same conditions as above. It can be observed that Re within the riser pipe is highest on 15th of June, as compared to 15th of March and 15th of September. The increase in heat flux input increases the Re within the riser pipe. Furthermore, it can be noticed that the Re increases, then decreases, depending on the increase/decrease in the heat flux input to the thermo-syphon.

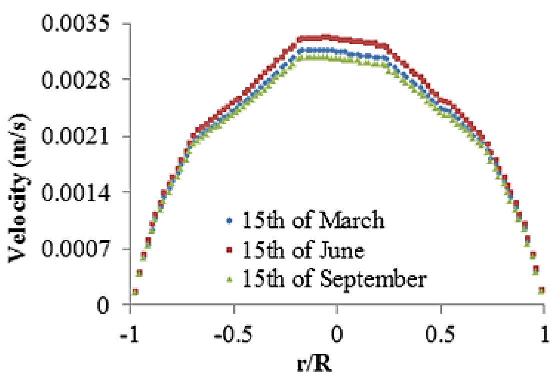

Figure 3. Velocity profiles within the middle riser pipe on different days of the year under thermal loading of a working day

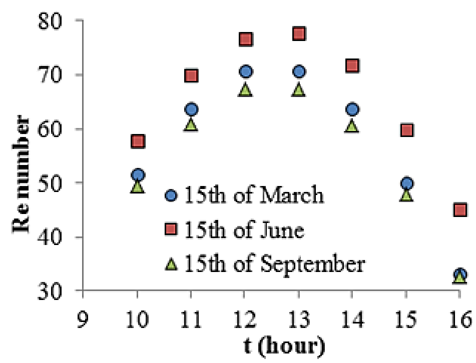

Figure 4. Reynolds number variations within the middle riser pipe on different days of the year under thermal loading of a working day

Figure 5 depicts static temperature distribution within the cross-section of the middle riser pipe for the three days of the year considered in the present study. The corresponding thermal loading condition that has been specified is that of the weekday. It can be clearly seen that the hot water occupies the upper-wall region of the riser pipe, whereas the cold water settles on the bottom of the pipe. This is because the density of the hot water reduces after absorbing solar energy, which causes it to rise above the more-dense cold water. It can be further noticed that the temperature within the riser pipe is highest on 15th of June as compared to 15th of March and 15th of September. This means that the working fluid's temperature increases significantly on the days when the heat flux input to the thermo-syphon is higher. It is evident that more heat flux provided to the riser pipes heats up the working fluid further.

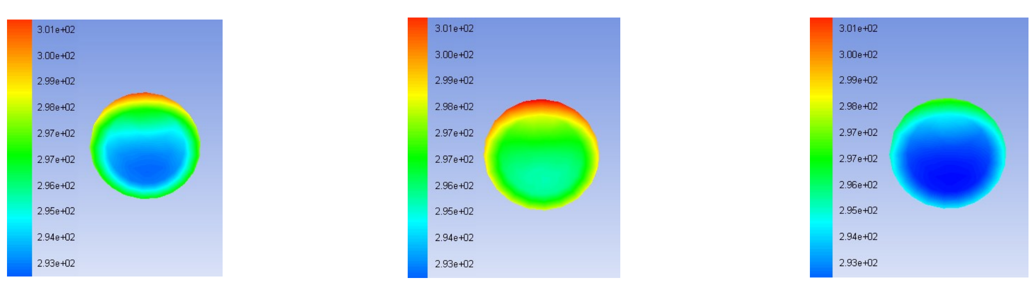

(a) **(b)** **(c)**

Fig. 5. Static temperature distribution within the middle riser pipe on (a) 15th March (b) 15th Jun (c) 15th September under thermal loading of a working day

Figure 6 depicts the static tempertaure profiles within the cross-section of the middle riser pipe. It can be clearly seen that the tempertaure of working fluid is higher in the near wall regions where the solar heat flux is directly in contact with the riser pipe's wall. Furthermore, increase in the heat flux input increases the temperature of the working fluid within the riser pipe.

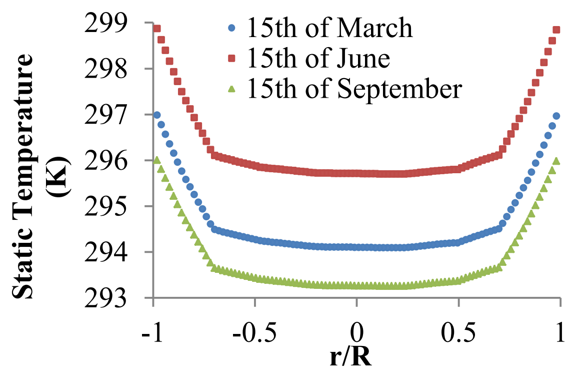

Figure 6. Static temperature variations within the middle riser pipe on different days of the year under thermal loading of a working day

3.2. Effect of thermal loading conditions on the performance of thermo-syphon

Figure 7 depicts the variation in flow velocity within the cross-section of the middle riser pipe, for the transient thermal loading conditions considered in the present study i.e. weekday and weekend. The corresponding heat flux input is of 15th of March. It has been observed that the velocity of the working fluid is primarily unaffected with the change in thermal loading patterns. This is due to the fact that the real-world thermal loading conditions vary only slightly, which results in insignificant flow variations. Hence, although it has been shown that the heat flux input has a significant effect on the velocity distribution within the riser pipes, thermal loading conditions have insignificant effects on it.

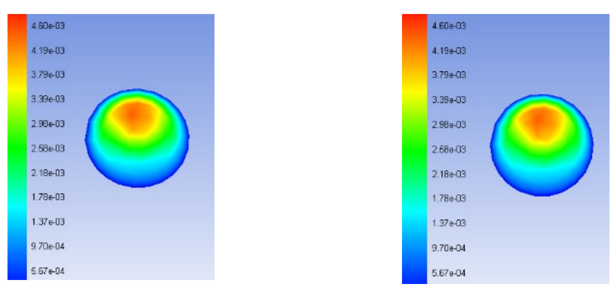

(a) **(b)**

Figure 7. Flow velocity variations within the middle riser pipe on 15th of June under (a) weekday loading and (b) weekend loading conditions

Figure 8 depicts the velocity profiles within the middle riser pipe for the various thermal loading conditions considered in the present study. It can be clearly seen that the working fluid's velocity within the riser pipe is unaffected by thermal loading. Furthermore, the velocity of working fluid is higher at the center of riser pipe for all the cases.

Figure 9 depicts the variations in Reynolds number within the cross-section of the middle riser pipe, on 15th of March, for the various thermal loading conditions considered in the present study. It can be clearly seen that Re within the riser pipe is unaffected by thermal loading conditions. Furthermore, it can be observed that Re increases/decreases with the increase/decrease in the heat flux input.

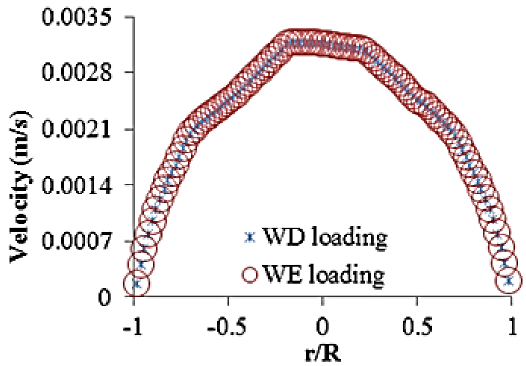

Figure 8. Velocity profiles within the middle riser pipe on 15th of March for various thermal loading conditions

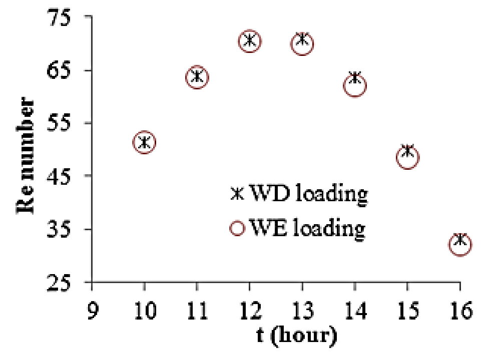

Figure 9. Reynolds number variations within the middle riser pipe on 15th of June for various thermal loading conditions

Figure 10 depicts the variation in static temperature of the working fluid within the cross-section of the middle riser pipe, for the transient thermal loading conditions considered in the present study. The corresponding heat flux input is of 15th of March. It has been observed that the static temperature of the working fluid is primarily unaffected by the changes in thermal loading patterns.

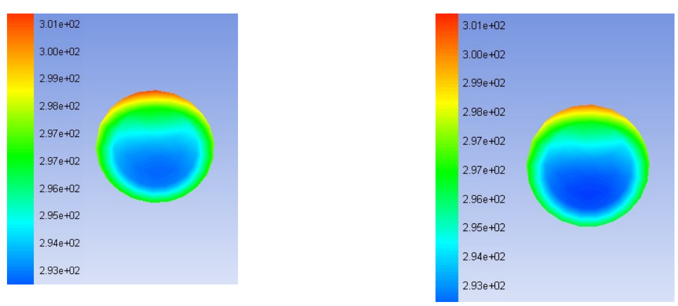

(a) (b)

Figure 10. Static temperature distributions within the middle riser pipe on 15th of March, under (a) weekday loading and (b) weekend loading

Figure 11 depicts the variations in the static temperaturte of the working fluid within the middle riser pipe, on 15th of March, for the various thermal loading considered in the present study. It can be clearly seen that working fluid's temperature within the riser pipe is unaffected by thermal loading conditions. Furthermore, the tempertaure of the working fluid is lowest in the center of riser pipe for all the cases.

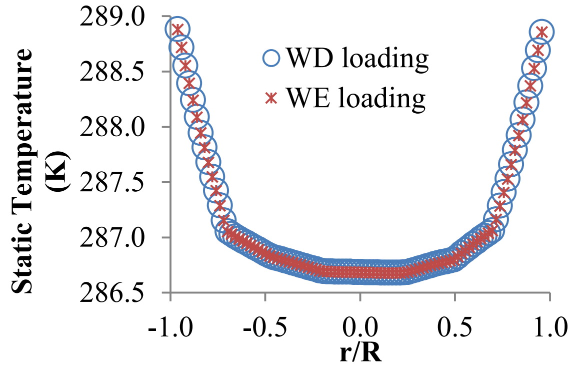

Figure 11. Static temperature variations within the middle riser pipe on 15th of March under (a) weekday loading and (b) weekend loading conditions

4. Conclusions

In the present study, the effects of transient heat flux inputs and thermal loading conditions have been numerically investigated on the flow distribution within the riser pipes of a closed-loop thermo-syphon. Different days of the year have been selected to cover a wide range of heat flux input, and both the weekday and weekend loading conditions have been considered. The results presented in this study suggest that the heat flux input affects the velocity and temperature of the working fluid within the riser pipe significantly, whereas, the thermal loading has negligible effects on both these parameters.

References

1. A Dehdakhel, M Rahimi and A Alsairafi, 'CFD modeling of flow and heat transfer in a thermo-syphon', International Communications in Heat and Mass Transfer Vol. 37 pp. 312–318, October 2009.
2. B Freegah, T Asim and R Mishra, 'Computational Fluid Dynamics based Analysis of a Closed Thermo-Siphon Hot Water Solar System', In: 26th International Congress of Condition Monitoring and Diagnostic Engineering Management, Helsinki, Finland, June 2013.
3. A Sato, I., Scalon, V. L., A Padilha, 'Numerical analysis of a modified evacuated tubes solar condenser', In: International Conference on Renewable Energies and Power Quality, March 2012.
4. J. Subramanian, S. Tamilkozhndu and T. Selvam, 'Experimental Studies on Variable Header Solar Water Heating System', 2nd International Conference on Mechanical, Production and Automobile, 2nd International Conference on echanical, Production and Automobile Engineering Singapore April 28-29 2012.
5. M Esen and H Esen, H, 'Experimental investigation of a two-phase closed thermosyphon solar water heater', Solar Energy, vol.79 (5), pp. 459-468, November 2005.
6. A Radhwan, G Zaki and A Jamil, 'Refrigerant-charged integrated solar water heater', Energy Research, vol. 14, pp. 421 – 432, 1990.
7. VC Agarwal and R Mishra, 'Optimal design of a multi-stage capsule handling multi-phase pipeline', international journal of pressure vessels and piping 75(1), 27-35, November 1998.
8. J Hu, Y Lee, T Blacker and J Zhu, 'Overlay Grid Based Geometry Cleanup', In IMR pp. 313-322 September 2002.
9. N Aung, and S Li, 'Numerical investigation on effect of riser diameter and inclination on system parameters in a two-phase closed loop thermo syphon solar water heater' Energy conversion and management, Vol 75, pp 25-35, November 2013.
10. ASHRAE Handbook, Fundamentals, 1985.
11. Z Sen, 'Solar energy fundamentals and modelling techniques' (pp. 36-37). Springer 2008.